Author response to Reviewer #1

We thank the reviewer for his insightful comments that helped significantly to improve the manuscript. Below, we respond to each of the specific comments (orange) and indicate how the comment will be addressed in the revised manuscript (*italic grey*).

The manuscript by Voigt et al. provides an important observation dataset of triple oxygen isotopic composition of water vapor, precipitation and surface/groundwater for one year in a forest in southern France. I believe this valuable dataset could be of interest to a broad scientific community working with stable water vapor isotopes. I also believe this is one of the very few studies focused on variations of the triple oxygen isotope composition in atmospheric water vapor. However, I have some concerns regarding this study, most of them are actually related to the measurement of 17O-excess in water vapor. That said, I'd like to suggest the manuscript to be deeply revised before continuing. Hope my comments can provide useful insights in this regards.

Major comment #1: Measurements of 17O-excess in atmospheric water vapor using Picarro CRDS analyzers are challenging. Even under optimal conditions, averaging for long time is required to discriminate a meaningful signal from instrumental noise. For L2140 analyzers, the typical 1-second Allan deviation is on the order of ~0.1–0.2 ‰ for both δ18O and δ17O, which results into ~100 per meg uncertainty in 17O-excess . Achieving a precision of ~10 per meg therefore generally requires 10–20 minutes of averaging.

These numbers are indicative, as each L2140 analyzer has specific performance. However, the key point is that such averaging reduces uncertainty only if the noise is white. Atmospheric water vapor at canopy scale is unlikely to exhibit white-noise characteristics on ~70 minute timescales due to e.g. turbulence and boundary-layer dynamics. In the presence of autocorrelation or colored noise, time averaging does not automatically reduce uncertainty as √N; instead, Allan deviation typically reaches a plateau or even increases at longer integration times in these conditions.

This limitation likely explains why measurements of 17O-excess in atmospheric water vapor are relatively rare and why cryogenic trapping followed by off-line analysis can still be a solution. In the context of this paper, the effective uncertainty of the reported 17O-excess values in the present study is likely underestimated, particularly for diurnal variations and vertical gradients between measurement heights that are of similar magnitude to the expected noise level.

I therefore recommend that the authors clarify (i) the noise structure of their vapor measurements, (ii) how the optimal averaging time was determined, and (iii) how effective uncertainty accounting for non-white noise and autocorrelation was estimated. The authors report that precision was determined using a Monte Carlo simulation. It is not clear on which assumptions the simulation is based on. Does the simulation account for uncorrelated noise and ~static signal (such as the one obtained by the A0211 vaporizer?). Or the simulation also accounts for e.g. turbulence noise spectrum?

I believe this is an important point to address, since the 17O-excess variability the authors observe is about the same order of magnitude of the uncertainty. This comment does not apply to the liquid measurement of precipitation, well and spring water.

We agree that the isotopic composition of atmospheric water vapor does not follow a white noise signal, but exhibits natural variability driven by turbulence and boundary layer dynamics. To assess how this natural variability influences measurement uncertainty and to determine the best integration interval, we calculated the Allan deviation for 24-hour isotope records obtained during the study period at our study site. In this analysis,

measurements from different sampling heights were combined because records longer than 90 min were not available for individual heights. Consequently, the calculated Allan deviation reflects not only temporal variability but also variability associated with vertical isotope gradients. The resulting Allan deviations are therefore likely higher than those derived from measurements at a single height. An example of the Allan deviation for June is shown in Fig. 1.

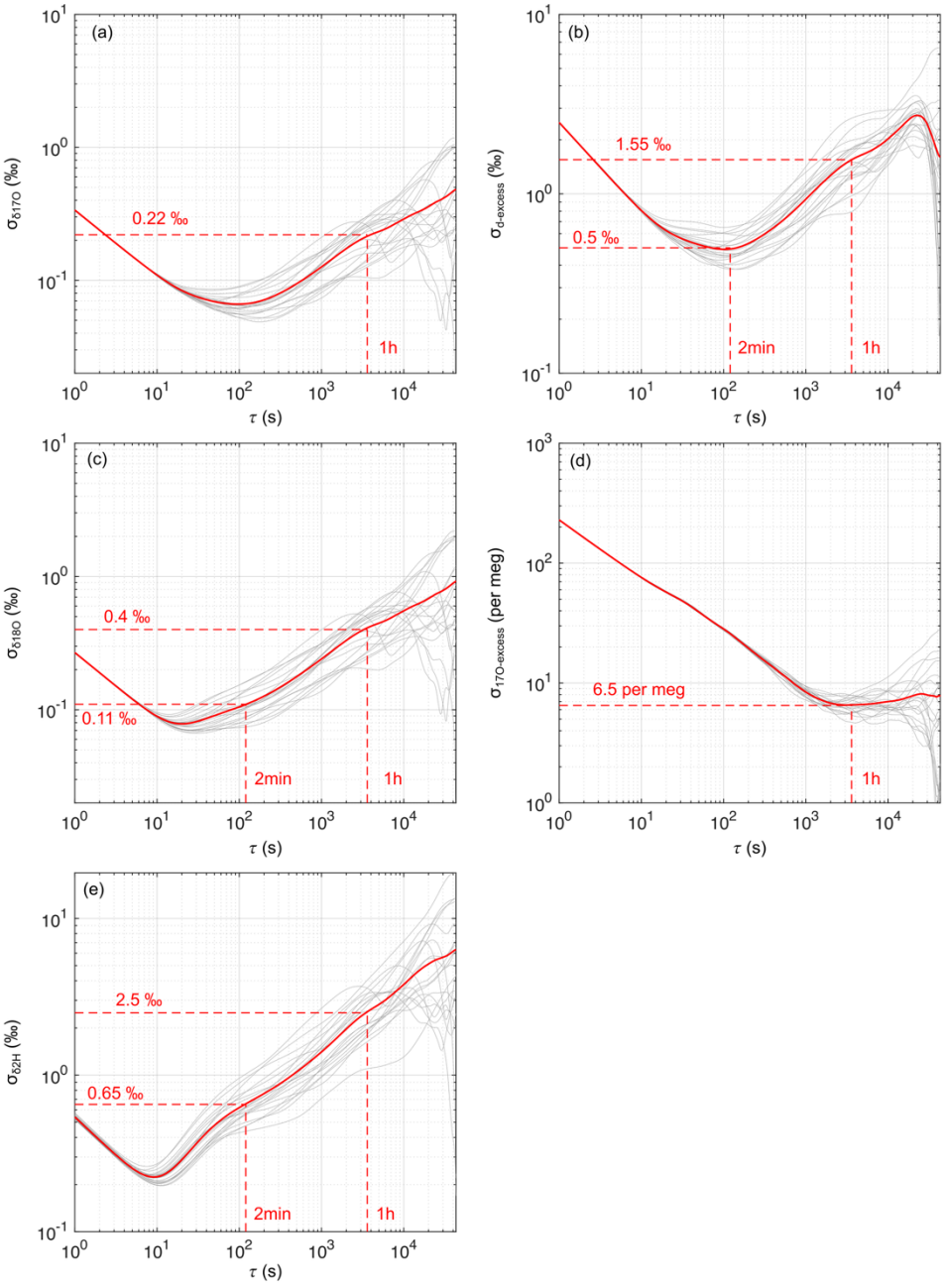

Fig. 1: Allan deviation σ for (a) $\delta^{17}O$, (b) $\delta^{18}O$, (c) $\delta^{2}H$, (d) d-excess and (e) ^{17}O-excess for 24-hour records of atmospheric water vapor at O_3HP gathered between 01.06.2021 and 30.06.2021. The red solid curve illustrates the mean Allan deviation. Dashed lines and associated numbers indicate the Allan deviation for 1 hour averaging time.

Fig. 1 indicates that the optimal integration interval for $\delta^{17}O$, $\delta^{18}O$, $\delta^{2}H$ and d-excess is on the order of a few minutes. For longer integration times, natural variability leads to larger Allan deviations. In contrast, the Allan deviation of ^{17}O-excess reaches a minimum of about 7 per meg at an averaging time of about 1 hour. Based on this result, we selected a 1-hour integration interval for our analysis.

The precision of the raw isotope data was estimated from these Allan deviation plots. A Monte Carlo simulation was performed to estimate the precision of the calibrated water vapor isotope data. Random normally distributed values were generated within the standard deviations of the raw $\delta^{18}O$, $\delta^{2}H$, and ^{17}O-excess values for (i) atmospheric water vapor, (ii) raw and (iii) reference standard measurements, and (iv) the coefficients describing the mixing-ratio dependency functions for $\delta^{17}O$, $\delta^{18}O$, and $\delta^{2}H$ of the two standards. For each randomly generated parameter set, the full calibration procedure described in the main text was applied. The precision of the calibrated atmospheric water vapor isotope data was estimated from the standard deviation of the calibrated value obtained in the Monte Carlo simulation.

To account for the mass-dependent relationship between $\delta^{17}O$ and $\delta^{18}O$, $\delta^{17}O$ was calculated from $\delta^{18}O$ and ^{17}O-excess, and the coefficients of the mixing ratio dependencu function for $\delta^{17}O$ were generated by applying the same standardized perturbation used for $\delta^{18}O$. Specifically, the generated coefficients for $\delta^{18}O$ wer converted to a z-score relative to heir mean and standard deviation, and these normalized deviations were then scaled and shifted using the $\delta^{17}O$ standard deviation and mean.

In the previous version, the minimum Allan deviations for $\delta^{17}O$, $\delta^{18}O$, $\delta^{2}H$ of raw atmospheric water vapor were mistakenly used instead of the Allan deviations corresponding to the 1-hour averaging interval. Using the corrected values, the simulation results suggest that the standard deviation of the calibrated data is approximately ± 0.2 ‰, ± 0.4 ‰, ± 2.7 ‰ and ± 15 per meg, and ± 4.2 ‰ for $\delta^{17}O$, $\delta^{18}O$, $\delta^{2}H$, ^{17}O excess, and d-excess, respectively. These standard deviations account for measurement uncertainty, uncertainty introduced by calibration, and natural variability over the 1-hour interval.

For comparison, we also performed Monte Carlo simulation using the SD for 2-min intervals, where the Allan deviation of d-excess is minimal (Fig. 1). The standard deviation of the raw $\delta^{18}O_{2min}$, $\delta^{2}H_{2min}$ and d-excess$_{2min}$ are 0.11 ‰, 0.65 ‰ and 0.5 ‰, respectively. Using these values in the simulation yields calibrated precisions over 2-min intervals of 0.12 ‰, 1.2 ‰ and 1.6 ‰, respectively, providing an estimate of the measurement and calibration uncertainty. We then re-calibrated the full atmospheric water vapor isotope record at 2-min intervals and averaged to 1-hour values to match the temporal scale of ^{17}O-excess. Figure 2 shows histograms of the standard deviation of $\delta^{18}O$, $\delta^{2}H$ and d-excess for the 1-hour mean value. The 95th percentiles of the observed range of SD are 0.6‰, 4 ‰ and 1.7 ‰ for $\delta^{18}O$, $\delta^{2}H$ and d-excess, respectively. These values primarily reflect natural variability over the 1hour interval.

We will revise the corresponding section in the manuscript accordingly. In addition, we will provide the MATLAB code used for the Monte Carlo simulation in a public data repository.

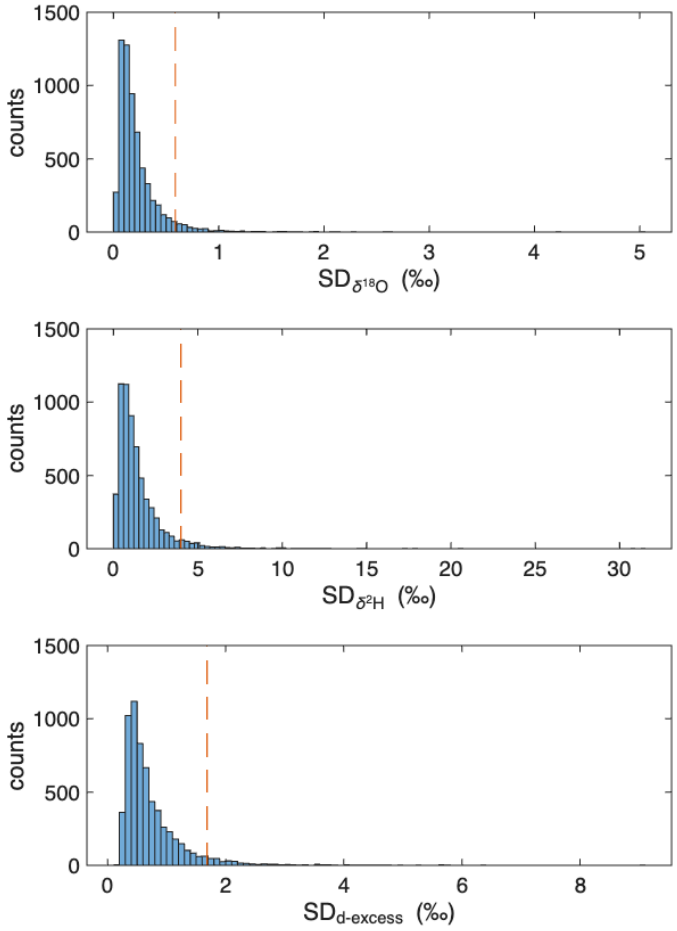

Figure 2: Histograms of the standard deviations of 1-hour mean values of $\delta^{18}O$, $\delta^{2}H$, and d-excess, obtained by averaging 2-minute calibrated atmospheric water vapor data. The SD of each 1-hour mean primarily reflects natural variability over the hour. Red dashed lines indicate the 95th percentile of the observed SD distribution (0.6 ‰, 4 ‰ and 1.7 ‰, respectively).

"The precision of raw isotope data was estimated from 24-hour in-situ measurements of atmospheric water vapor at O3HP in June 2021 using Allan deviation analysis. While the optimal integration time for $\delta^{17}O$, $\delta^{18}O$, $\delta^{2}H$ and d-excess is on the order of a few minutes, the Allan deviation of ^{17}O-excess reaches a minimum (~7 per meg) at an averaging time of about 1 hour. Based on this, a 1-hour integration interval was chosen for analysis. Allan deviations at this interval were 0.2 ‰ for $\delta^{17}O$, 0.4 ‰ for $\delta^{18}O$, 2.5 ‰ for $\delta^{2}H$, 1.6 ‰ for d-excess and 7 per meg for ^{17}O-excess (Fig. AX), reflecting both measurement uncertainty and natural variability.

To assess the precision of calibrated data, a Monte Carlo simulation was applied following Voigt et al. (2022). In 100 000 iterations, random normally distributed values were generated within the standard deviations of (i) raw $\delta^{18}O_V$, $\delta^{2}H_V$ and $^{17}O\text{-excess}_V$, (ii) the coefficients of the mixing ratio dependency functions and (iii-iv) the measured and reference values of $\delta^{18}O$, $\delta^{2}H$ and ^{17}O-excess of the two standards. In each iteration, raw atmospheric values were calibrated following the above-described procedure. The simulation indicated standard deviations of the calibrated values of approximately ± 0.2 ‰, ± 0.4 ‰, ± 2.7 ‰ and ± 15 per meg, and ± 4.2 ‰ for $\delta^{17}O$, $\delta^{18}O$, $\delta^{2}H$, ^{17}O-excess, and d-excess, respectively.

To better estimate measurement uncertainty, the Monte Carlo simulation was repeated using the SD of 2-min intervals, where d-excess exhibits minimal Allan deviation (Fig. AX). The raw SD were 0.11 ‰, 0.65 ‰ and 0.5 ‰ for $\delta^{18}O_{2min}$, $\delta^{2}H_{2min}$ and d-excess$_{2min}$, respectively, yielding simulated calibrated precisions of 0.12 ‰, 1.2 ‰ and 1.6 ‰ over 2-min intervals."

Major comment #2: The authors report water vapor observations using a multiple-inlet system (0.4 m, 1.5 m, 3.5 m, and 12.5 m). However, several key aspects of the sampling configuration are insufficiently described. In particular, the total length of the inlet lines is not stated, and it is not clear whether the individual lines are flushed continuously when not connected to the Picarro via the port distribution manifold. It is also unclear whether the analyzer is connected directly to the inlet distribution manifold or whether an intermediate volume is present (e.g. a buffer or the A0211 vaporizer). Moreover, the reported analyzer flow rate (~0.4 mL/min) is low for such analyzers. My concern is that the combination of potentially unflushed inlet lines and low analyzer flow rates have impact on residence time and memory effects within the sampling system, resulting into signal smoothing and carryover between successive inlets. This is especialy true when switching between heights characterised by different humidity and isotopic composition. With the information reported by the authors, it is difficult to assess whether the (lack of) observed variability between inlets reflect true atmospheric variability or are partly influenced by sampling-system artefacts. A long-term averaging (e.g. daily or even seasonal) might also have flattened any difference in isotopic composition of water vapor between the inlets at different heights. I recommend that the authors provide a more detailed description of the inlet configuration and flow scheme, e.g. with a diagram, and, if possible, include quantitative tests or estimates of memory effects associated with inlet switching.

From bottom to top, the inlet lines were approximately 11.5 m, 15 m, 20 m, and 32 m long. Each line was continuously flushed with a flow rate of 5 L min^{-1}. The port distribution manifold is connected to the vaporizer, which is coupled to the analyzer. The instrument subsampled the inlet lines with a flow rate of 35 mL min^{-1}. We believe that residence times and the memory effect is minimized by the high flush rate. The residence time was less than 20s for the longest tube. However, we discarded the first 10 min of each line measurement to minimize any memory effect. We added this information in the revised version. In addition, we provide a figure illustrating the experimental setup (see below).

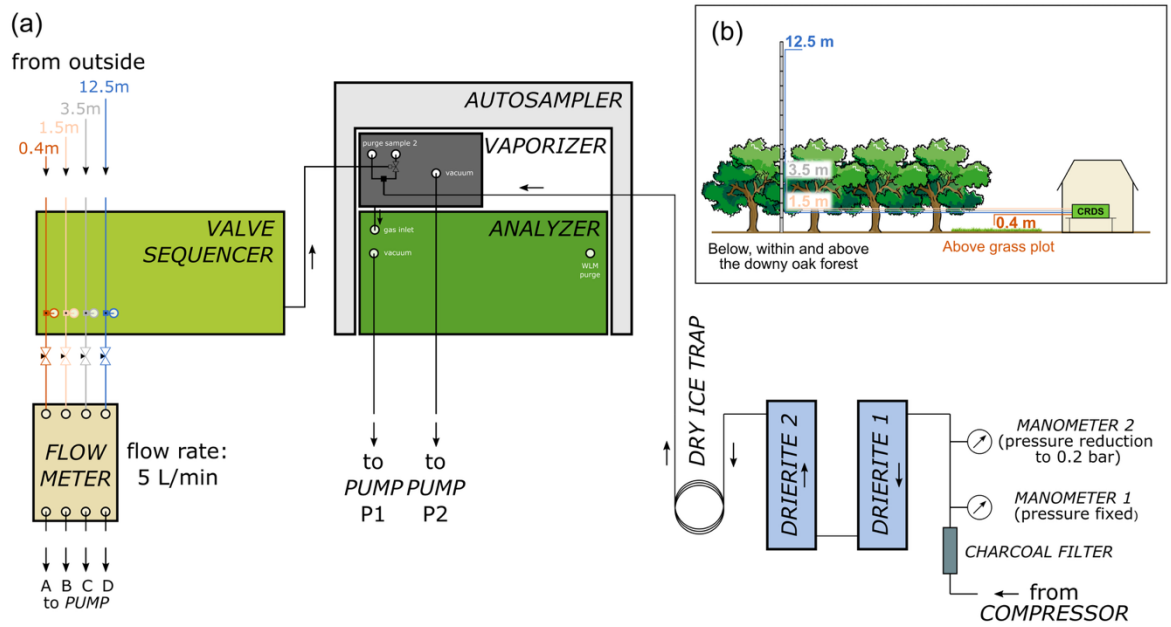

Major comment #3: The statistical analysis of air-parcel origins based on back-trajectory frequency does not directly identify moisture sources of precipitation or boundary-layer water vapor origin. In particular, in Section 3.6 (lines 315–320), the attribution of moisture sources remains qualitative, as the analysis considers only the geographic origin of air masses and not the actual moisture exchange of air parcels with the ocean surface (evaporation) or land (evapotranspiration).

This distinction is important because air-mass origin does not necessarily correspond to moisture source, strongly limiting boundary layer water vapor mass-balance calculation/speculations. During atmospheric transport, water vapor undergo several processes, to mention a few: condensation, re-evaporation, mixing, local evapotranspiration, etc. All of these processes substantially modify the isotopic composition of water vapor. Consequently, caution is required when attributing isotopic signatures to specific moisture sources based solely on back trajectories, particularly for δ18O and δD, whose variability is influenced by several factors such as local temperature and convective activity. In this context, d-excess and likely 17O-excess (as suggested by the manuscript itself) represents a more robust parameter for investigating moisture source conditions.

A more statistically and physically consistent approach would be to combine back trajectories with isotopic observations at the O3HP site, for example using concentration weighted trajectories (implemented in the HYSPLIT framework employed by the authors) which have proven effective in previous studies in the Mediterranean region (e.g. Salamalikis et al., 2015). Another option would be to use a Lagrangian moisture diagnostics that explicitly identify moisture uptake along trajectories (e.g. following Sodemann et al., 2008, as mentioned by the authors in the conclusion). The latter would provide a more rigorous basis for source attribution and mass-balance. Such approach have been successfully applied to disentangle the drivers of water vapor d-excess variability in continental boundary layers (e.g. Aemisegger et al., 2014).

At present, the message conveyed in lines 321–329 is unclear. The interpretation would benefit from rephrasing and acknowledging the limitations of the source attribution method used in this study. A similar caution applies to discussion section 4.1.

Finally, given the proximity of the study site to the Mediterranean Sea, one might also expect a stronger influence from the western Mediterranean and central Europe. The seasonal source decomposition presented by Sodemann and Zubler (2010; their Fig. 8) could serve as a useful

reference framework for contextualizing the results (although the latter paper is focused on precipitation only).

The authors should clarify the distinction between air-mass pathways and moisture sources, and edit the interpretation accordingly.

We implemented now a Lagrangian moisture source diagnostic following Sodemann et al. (2008). Along each 168-h backward trajectory, positive increments in specific humidity ($\Delta q > 0$) calculated at 6-hour intervals were interpreted as moisture uptake from the underlying surface. Each uptake location was assigned to the midpoint of the corresponding trajectory segment. Only uptake events exceeding 0.2 g kg^{-1} and occurring below 1.5 times the planetary boundary layer height were considered, consistent with Sodemann et al. (2008), in order to restrict moisture contributions to boundary-layer exchange processes. Each uptake event was weighted by its relative contribution to the final specific humidity at the study site. If a decrease in specific humidity ($\Delta q < 0$), interpreted as precipitation loss, occurred downstream of one or more uptake events, the contributions of the preceding uptakes were proportionally reduced to account for moisture removal, following the conservation framework described in Sodemann et al. (2008). This procedure yields, for each trajectory k, the fractional contribution $\tau_{(ij)k}$ of a grid cell (i,j) to the final humidity at the study site.

Subsequently, we applied a modified Concentration Weighted Trajectory (CWT) approach after Salamalikis et al. (2015). A spatial grid of 2° × 2° resolution was defined over the study domain. Instead of weighting the isotopic composition measured at the study site by the residence time in each grid cell, we weighted it by the previously derived fractional moisture contribution $\tau_{(ij)k}$. The isotopic signature assigned to each grid cell (i,j) was computed as:

$$C_{ij} = \frac{\sum_{k=1}^{N} \tau_{ijk}\ C_k}{\sum_{k=1}^{N} \tau_{ijk}}$$

Where C_k is the isotopic composition ($\delta^{18}O$, d-excess, or ^{17}O-excess) measured upon arrival of trajectory k at the study site, and τ_{ijk} is the fractional moisture contribution of grid cell (i,j) to trajectory k.Thus, C_{ij} represents the moisture-contribution-weighted isotopic composition associated with evaporation from grid cell (i,j).

For regional interpretation, we aggregated grid cells into eight predefined source regions after Sodemann and Zuber (2010). (NW = Northwest North Atlantic, NE = Northeast North Atlantic, SW = Southwest North Atlantic, SE = Southeast North Atlantic, A = Arctic and Nordic Seas, CE = Central Europe, MW = Western Mediterranean, ME = Eastern Mediterranean). To focus on oceanic moisture sources, only grid cells located over ocean surfaces were considered. Land areas were maks using the MATLAB-built in shapefile *landareas*.

The results of the moisture source analysis are illustrated in Fig. 3 and 4 for atmospheric water vapor and Fig. 5 and 6 for precipitation. Moisture is mainly derived from the NE North Atlantic and the Western Mediterranean with minor contributions from SE North Atlantic, NW, North Atlantic and Central

Europe (see Table 1). For precipitation, the Western Mediterranean is the dominant moisture source.

Table 1 also shows the mean isotopic composition of atmospheric water vapor and precipitation derived from the eight defined oceanic moisture source region sectors. Consistently with our previous intepretation, there is no significant difference in d-excess and ^{17}O-excess of atmospheric water vapor and precipitation derived from the North Atlantic and Western Mediterranean sources. The Eastern Mediterranean shows higher d-excess$_V$ and ^{17}O-excess$_V$ values. However, its contribution to on-site moisture is insignificant over the study period. This quantitative analysis will be implemented in the revised version of the manuscript and the Results and Discussion section will be updated accordingly.

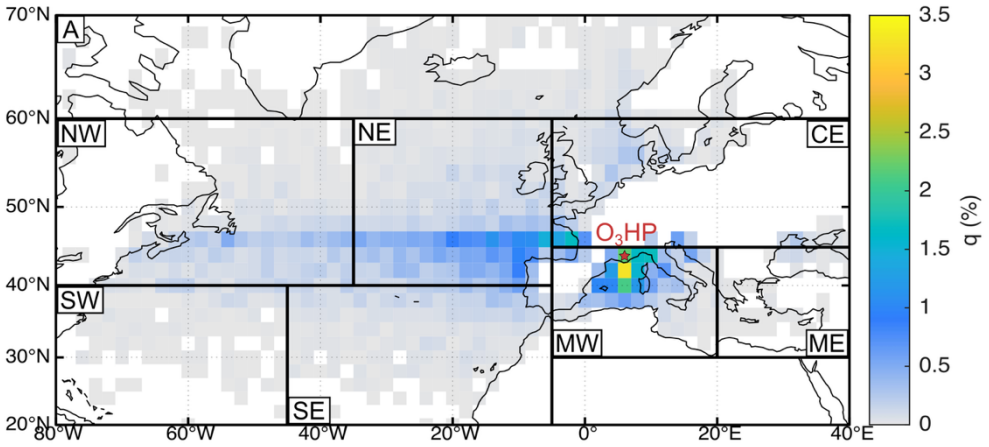

Figure 3: Annual mean oceanic moisture sources for atmospheric water vapor at O_3HP. Shading: Relative contribution of evaporation from respective grid cell to the final specifc humidity of each trajectory.

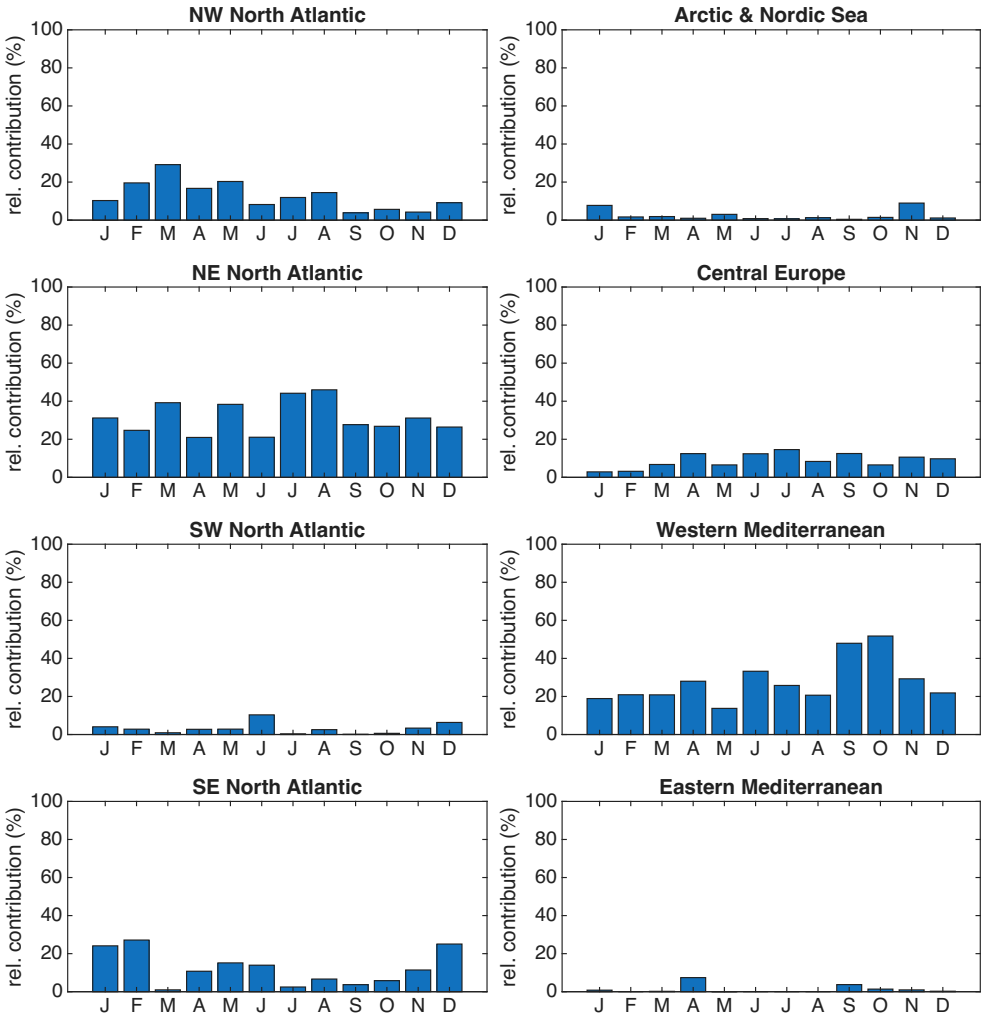

Figure 4: Relative contributions from the four oceanic moisture source regions (% of final specific humidity).

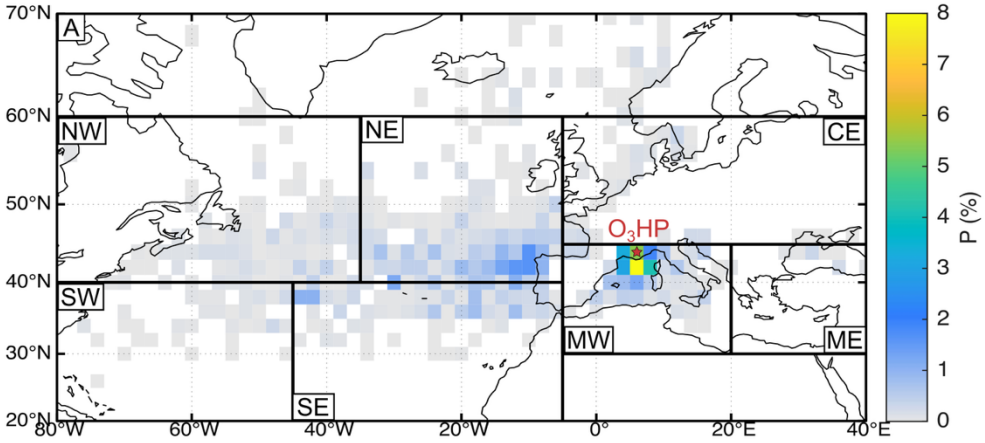

Figure 5: Annual mean oceanic moisture sources for precipitation at O_3HP. Shading: Relative contribution of evaporation from respective grid cell to diagnosed precipitation at O_3HP.

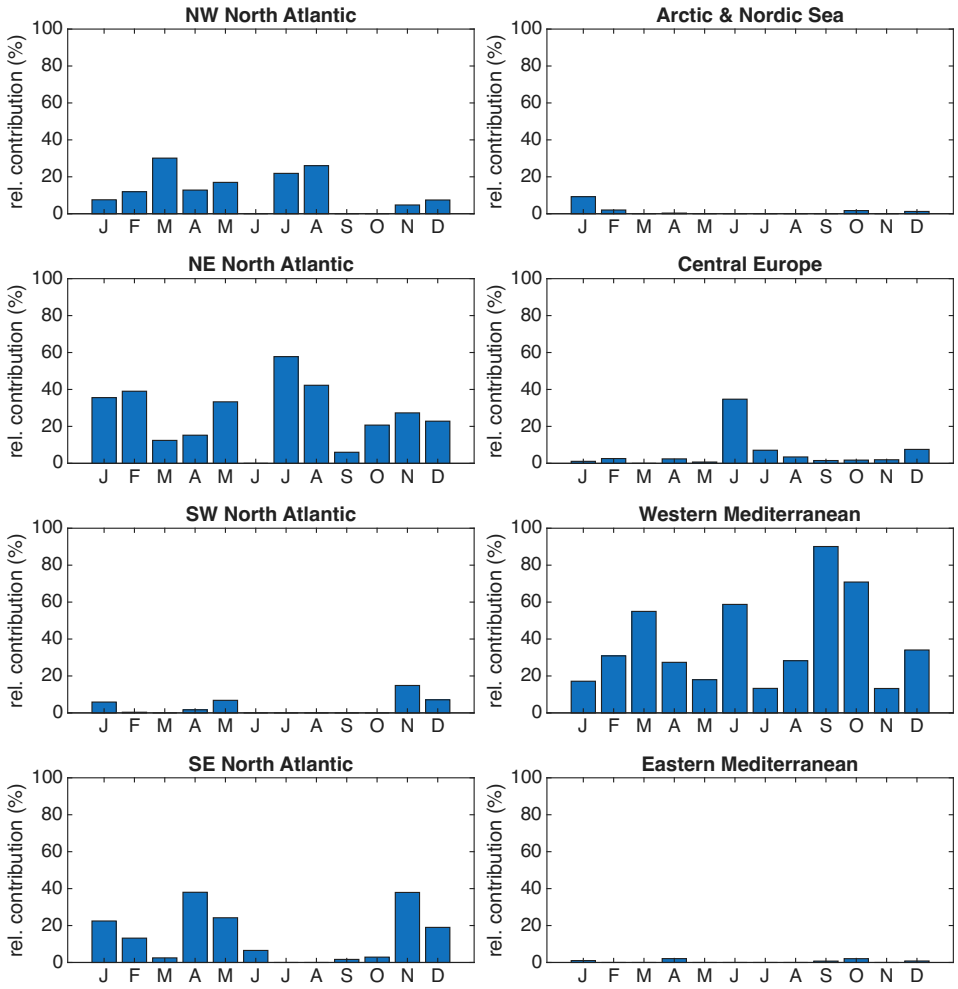

Figure 6: Relative contributions from the eight oceanic moisture source region sectors (% of accounted precipitation).

Table 1: Isotopic composition of atmospheric water vapor and precipitation derived from the four defined oceanic moisture source regions.

Moisture source region	d18OV		d-excessV		17O-excessV		relative contribution (%)
	AV	SD	AV	SD	AV	SD	
Atmospheric water vapor							
NW North Atlantic	-16.1	4.1	11.9	3.4	26	8	12
NE North Atlantic	-15.6	3.5	11.2	2.8	25	6	32
SW North Atlantic	-15.0	3.4	11.0	2.3	27	7	3

SE North Atlantic	-14.8	4.8	9.0	3.0	27	9	11
Arctic and Nordic Sea	-16.6	7.6	10.9	6.0	25	13	2
Central Europe	-17.4	4.7	13.2	3.8	26	8	10
Western Mediterranean	-14.4	4.1	11.0	3.2	25	7	29
Eastern Mediterranean	-17.1	4.6	13.9	5.1	36	13	1
Precipitation							
NW North Atlantic	-8.2	2.4	13.4	3.6	30	11	8
NE North Atlantic	-9.0	3.8	11.8	3.4	32	13	25
SW North Atlantic	-8.7	2.1	12.0	2.1	32	4	4
SE North Atlantic	-8.6	2.8	11.9	3.4	33	6	18
Arctic and Nordic Sea	-12.0	6.6	13.1	2.7	42	17	2
Central Europe	-7.3	4.1	9.5	8.7	26	14	3
Western Mediterranean	-7.5	2.5	11.2	3.0	27	7	40
Eastern Mediterranean	-8.5	8.1	9.2	13.0	30	25	1

Aemisegger, F., Pfahl, S., Sodemann, H., Lehner, I., Seneviratne, S. I., & Wernli, H. (2014). Deuterium excess as a proxy for continental moisture recycling and plant transpiration. _Atmospheric Chemistry and Physics_, _14_(8), 4029–4054. https://doi.org/10.5194/acp-14-4029-2014

Salamalikis, V., Argiriou, A. A., & Dotsika, E. (2015). Stable isotopic composition of atmospheric water vapor in Patras, Greece: A concentration weighted trajectory approach. _Atmospheric Research_, _152_, 93–104. https://doi.org/10.1016/j.atmosres.2014.02.021

Sodemann, H., Schwierz, C., & Wernli, H. (2008). Interannual variability of Greenland winter precipitation sources: Lagrangian moisture diagnostic and North Atlantic Oscillation influence. _Journal of Geophysical Research Atmospheres_, _113_(3), 1–17. https://doi.org/10.1029/2007JD008503

Sodemann, H., & Zubler, E. (2010). Seasonal and inter-annual variability of the moisture sources for alpine precipitation during 1995-2002. _International Journal of Climatology_, _30_(7), 947–961. https://doi.org/10.1002/joc.1932

Minor comments:

- Abstract L20: Please clarify whether the authors refer to evaporation or evapotranspiration.

In principle, ^{17}O-excess is driven by evaporation processes. Evaporation decreases $\delta^{18}O_V$ and increases d-excess$_V$ and ^{17}O-excess$_V$, wheras plant transpiration, which is assumed to be non-fractionating relative to soil water (Galewsky et al., 2016 and references therein), should increase $\delta^{18}O_V$ but have little impact on d-excess$_V$ and ^{17}O-excess$_V$. Our results show that, on seasonal

scale, $^{17}O\text{-}excess_V$ reflects climate conditions during evaporation in oceanic moisture sources. On the other hand, day-night variations in $^{17}O\text{-}excess_V$ reflect the combination of several daily processes including soil water evaporation, plant transpiration, dewfall evaporation, entrainment of remnant of the convective boundary layer, and isotope exchange between leaf and soil waters and the atmosphere. The conclusion and the abstract will be reworked to account for the changes in the section discussion section on terrestrial moisture recycling in the manuscript.

- L104-115: I believe three mixing ratio sensitivity experiments are sufficient, assuming no change in the experimental setup during the study period. Please also report how may calibrations were performed (daily, weekly, etc). Was the water vapor Picarro also calibrated for the mixing ratio?

Indeed, we analysed liquid standards weekly at four water mixing ratios (3000, 7000, 11000 and 17000 ppmv). As the results were consistent with the mean of the more highly resolved water mixing ratio functions, we neglected the measurements at 3000, 7000 and 17000 ppmv, used only the measurements at 11000 ppmv for calibration and the mean functions for mixing ratio dependency correction. We specify this now in the revised version.

"The calibration protocol of atmospheric water vapor isotope data is described in detail in Voigt et al. (2023). In brief, three liquid water standards that covered the expected isotopic range of atmospheric water vapor at the study site were analyzed weekly at four water mixing ratios (3000 ppmv, 7000 ppmv, 11000 ppmv and 17000 ppmv) using an autosampler system (A0325, Picarro Inc., California, USA) coupled to a high-precision vaporizer (A0211, Picarro Inc., California, USA). The liquid standards were injected in a dry air stream, produced by a lubricated mobile air compressor (MONTECARLO FC2, ABAC air compressors, Italy), further dried using two drierite columns combined with a dry ice trap. Using dry ambient air as carrier gas for calibration of atmospheric water vapor isotope measurements is crucial to avoid any potential matrix effect (Voigt et al., 2022).
The weekly mixing ratio dependencies were found to be consistent with the mean of three more highly resolved mixing ratio dependency functions. Therefore, the means of the more highly resolved mixing ratio dependency functions were used for mixing ratio dependency correction, while the weekly standard measurements at 11000 ppmv were used for calibration. In detail, raw isotope compositions of the liquid standards of four consecutive measurement runs were averaged and subsequently corrected to the water mixing ratio of the measured atmospheric water vapor. The standards with the lowest and the highest isotopic values were used for two-point calibration on VSMOW-SLAP scale, while the third standard with an intermediate isotopic composition served as quality control."

- L138: please correct 0.4 - 10 m agl.

The ICOS Tower measured air temperatures at 10, 50 and 100 m. Even using temperatures at higher elevations does not significantly influence the results. We specify this now.

"Note that using different air temperatures measured between 0.4–100 m agl does not significantly influence the results."

- L168-169: The sentence is unclear as currently written. Please rephrase.

With the implementation of the quantative moisture source analysis precipitation events are not classified anymore per moisture source region but rather moisture sources per precipitation sample has been quantified. The text in the revised version will be adjusted accordingly.

- I suggest framing the geographical location of the study area more clearly in the context of the Mediterranean basin and the Atlantic Ocean. This information is currently discussed later in the manuscript (see Fig. 4), but it would be helpful to introduce it earlier, together with the description of the study site. It would be nice to have a single Figure showing the geographical location of the study area and a photo of the study site. Given that surrounding vegetation and landscape seem to be important actors in isotope processes at the ecosystem scale, visual context would be valuable. More on this, I have googled the coordinates and the observatory seems to be on a mountain slope. Do the authors expect wind direction or local circulation (e.g. mountain–valley breeze systems) to influence local moisture sources or boundary-layer dynamics?

The region exhibits geological folding characteristic of the Alpine orogeny. The observatory is situated on a 15 km² raft foundation inclined at 2–4%, a configuration typical of the broader surroundings rather than a discrete topographic peak or ridge. Thermal turbulence and updraft manifesting is anticipated but uniformly distributed across the surrounding >20 km radius. While valleys may exhibit marginally elevated humidity episodically, open water bodies are negligible—limited to ephemeral streamlets—owing to the karstic limestone lithology, which facilitates rapid infiltration; most streamlets desiccate promptly post-precipitation. We will add a map with the study location and a photo from the study site.

Fig. 7: Left: View of understory and atmospheric water vapor measurements above the grass plot (0.4m agl). Right: View above the downy oak forest canopy with the mast and installed tubes for atmospheric water vapor measurent on top.

- A schematic representing the measurement setup is missing. A simple diagram illustrating the measurement setup would greatly improve clarity.

A figure representing the measurement setup will be provided in the revised version (see above).

- Modeling the isotopic evaporation flux (L180): if the authors refer to the exponent n controlling the ratio of water vapor isotopolues diffusivities in air (see, e.g eq. 17 in Horita et al., 2008) it should be noted several works show smaller effective values of n, following e.g. Duetsch et al. (2025, Figure 2) and experimental evidences in references therein.
Horita, J., Rozanski, K., & Cohen, S. (2008). Isotope effects in the evaporation of water: A status report of the Craig-Gordon model. _Isotopes in Environmental and Health Studies_, _44_(1), 23–49. https://doi.org/10.1080/10256010801887174
Duetsch, M., Fairall, C. W., Blossey, P. N., & Fiorella, R. P. (2025). _A new theoretical framework for parameterizing nonequilibrium fractionation during evaporation from the ocean_. https://doi.org/10.22541/essoar.174785883.32412797/v1

The turbulence coefficient is an empirical parameter that cannot be directly measured. We choose a value of 0.33, which is at the upper end of previously reported values. Using lower values implies lower kinetic fractionation during evaporation and thus lead to lower d-excess and ^{17}O-excess values in the resulting water vapor. We now specify this in the revised version.

"Further, we used a turbulence coefficient of 0.33, which is at the upper end of previously reported values for open-ocean evaporation (see, e.g., Gat, 1996; Pfahl & Wernli, 2008; Uemura et al., 2010, Duetsch et al., 2025). The turbulence coefficient is an empirical parameter that quantifies the contribution of molecular diffusion to the total kinetic fractionation during evaporation. Several studies have attempted to constrain this parameter empirically (e.g., Pfahl and Wernli, 2008; Uemura et al., 2010; Zannoni et al., 2022) and to develop theoretical frameworks (Horita et al., 2008; Xia et al. 2023; Duetsch et al., 2025). Lower turbulence coefficients reflect lower kinetic fractionation during evaporation and therefore lower d-excess and ^{17}O-excess values in the evaporated water vapor."

- Figure 1 c: evidence of fractionated precipitation during summertime (negative d-excess)

Yes, this is an indication for re-evaporation of the precipitation during falling as analysed in detail in Section 3.4 and discussed in Section 4.1.

- L284: For δ18O and δD might be of interest of comparing with similar studies that were performed for long time-intervals in different climate settings such as Chen et al., 2024, Deshpande et al. 2010.

We discuss the isotopic (dis)equilibrium between precipitation and atmospheric water vapor in Section 4.5. We will add a short phrase comparing our results to different climate settings where rain re-evaporation effects.

"In monsoon areas, $\delta^{18}O$ and $\delta^{2}H$ of atmospheric water vapor can be lower than suggested by isotope equilibrium due to sub-cloud re-evaporation (Desphande et al., 2010; Landais et al., 2010; Wen et al., 2010; Chen et al., 2024)."

Chen, M., Gao, J., Luo, L., Zhao, A., Niu, X., Yu, W., Liu, Y., & Chen, G. (2024). Temporal variations of stable isotopic compositions in atmospheric water vapor on the Southeastern Tibetan Plateau and their controlling factors. _Atmospheric Research_, _303_, 107328. https://doi.org/10.1016/j.atmosres.2024.107328
Deshpande, R. D., Maurya, A. S., Kumar, B., Sarkar, A., & Gupta, S. K. (2010). Rain-vapor interaction and vapor source identification using stable isotopes from semiarid western India. _Journal of Geophysical Research Atmospheres_, _115_(23), 1–11.

- Figure 4: The caption length should be reduced and discussion of the results should be moved from the caption to the main text (sect. 3.4)

We reduced the length of the caption. It now reads as follows. The removed information was already provided in the discussion so that we did not change the main text.

"Figure 4: Isotope difference (Δ) between water vapor estimated from isotope equilibrium with precipitation (Veq) and amount-weighted atmospheric water vapor measured at 12.5 m above ground level (V) for each precipitation event in 2021. Data is coloured according to season. The blue-shaded area indicates samples for which the equilibration between precipitation and near-surface atmospheric water vapor is likely incomplete. Precipitation samples that correspond to data falling within the grey-shaded area are likely affected by re-evaporation during fall through the air column."

- L342-346: The discussion of NAO phases and water vapor isotope composition is interesting but only briefly mentioned. It is worth noting that other studies identified strong links between NAO phases, weather regimes and ground-level water vapor and precipitation isotope composition e.g.: Deininger et al. (2016) for precipitation over continental Europe in winter, Zannoni et al. (2019) for water vapor at ground level in the Mediterranean basin. A short expansion or contextualization would strengthen this section.

Deininger, M., Werner, M., & McDermott, F. (2016). North Atlantic Oscillation controls on oxygen and hydrogen isotope gradients in winter precipitation across Europe; implications for palaeoclimate studies. _Climate of the Past_, _12_(11), 2127–2143. https://doi.org/10.5194/cp-12-2127-2016
Zannoni, D., Steen-Larsen, H. C., Stenni, B., Dreossi, G., & Rampazzo, G. (2019). Synoptic to mesoscale processes affecting the water vapor isotopic daily cycle over a coastal lagoon. _Atmospheric Environment_, _197_(March 2018), 118–130.

In the revised version, we will expand the Methods section to include the motivation of the assessment of the correlation between weather regimes and the isotopic composition of precipitation/atmospheric water vapor as follows:

"Synoptic atmospheric variability over Europe can be characterized using weather regimes (Cassou, 2008; Cassou et al., 2005; Michelangeli et al., 1995; Vautard,

1990). Previous studies have demonstrated strong positive correlations between $\delta^{18}O_P$ and $\delta^{2}H_P$ and the NAO index (Baldini et al., 2008; Field, 2010; Deininger et al., 2016; Zannoni et al., 2019). In addition, Zannoni et al. (2019) reported a negative correlation between d-excess and the NAO index at a coastal lagoon in Venice. These correlations are strongest in central Europe but are often weaker in mountainous and circum-Mediterranean regions. Local orographic effects and moisture recycling have been put forward as factors that could mitigate the impact of the NAO, but without any evidence. (Baldini et al., 2008).
Here, we identify the impact of dominant weather regimes on the isotopic composition of atmospheric water vapor and rainfall in order to assess the potential of the region's paleoclimate archives."

Further, we will add a Discussion Section on the relationship between the weather regimes and the isotopic compositon of atmospheric water vapor and precipitation containing the following information:
"The absence of correlation between the weather regimes and the isotopic composition of vapor and precipitation is probably due to the combined influence of multiple moisture sources weakly isotopically contrasted as presented in Section 3.6. In addition, local moisture recycling may further modify the isotopic signal of atmospheric water vapor and, thus, precipitation, as previously suggested for the circum-Mediterranean region (Baldini et al., 2008). It is also possible that the isotopic composition of near-surface atmospheric water vapor differs slightly from that of the free troposphere due to ground roughness, convection, mixing processes in the planetary boundary layer (Griffis et al., 2016; Salmon et al., 2019; Tada et al., 2021)."

- L346-347: Water vapor isotopic composition measured near the surface can be representative of the boundary layer, but its variability may be modulated by ground roughness/homogeneity, convection, mixing, climate and weather regime, time of the day among the most important. Aircraft and tall-tower measurements provide strong evidence in this regard: see e.g. Salmon et al. (2019), Griffis et al. (2016)

We thank the reviewer for this clarification. This will be specified in the revised version in the new discussion section on the realtionship between weather regimes and isotopic compositions of vapor and precipitation (see above).

Griffis, T. J., Wood, J. D., Baker, J. M., Lee, X., Xiao, K., Chen, Z., Welp, L. R., Schultz, N. M., Gorski, G., Chen, M., & Nieber, J. (2016). Investigating the source, transport, and isotope composition of water vapor in the planetary boundary layer. _Atmospheric Chemistry and Physics_, _16_(8), 5139–5157. https://doi.org/10.5194/acp-16-5139-2016
Salmon, O., Welp, L. R., Baldwin, M., Hajny, K., Stirm, B., & Shepson, P. (2019). Vertical profile observations of water vapor deuterium excess in the lower troposphere. _Atmospheric Chemistry and Physics_, _19_(17), 11525–11543. https://doi.org/10.5194/acp-19-11525-2019

- L391-394, L407-409, Figure 5.i: what the 17O-excess composition of the seawater source should be to agree with observed atmospheric water vapor value?

As specified in the discussion section, the isotopic composition of the source water of evaporation influences the isotopic composition of the evaporated

water vapor. If the seawater would have 5 instead of the assumed -5 per meg, the ^{17}O-excess of the evaporated water vapor would be 10 per meg higher.

- L427: compounded forms such as "kppmv" are not recommended under metrology standards. Just reports "thousands of ppmv" or simply "< 4000 ppmv"

This will be adjusted in the revised version.

- L428-430: Rayleigh distillation assumes isotopic equilibrium. These conditions are applicable inside a cloud (100% RH), but not for most of the conditions reported in this study.

We state here that the $\delta^{18}O$ of water vapor at cloud height (1000-2000m above ground) is likely depleted relative to near-surface water vapor. This has been observed in aircraft and tall-tower measurements and attributed to Rayleigh fractionation during adiabatic ascent (Sodemann et al., 2017; Salmon et al., 2019). The vertical profiles can be modified transport, mixing and cloud processes within the boundary layer as the reviewer also outlined above. However, the general tendencies for $\delta^{18}O$ and d-excess remain.

- L590 (data availability) PANGAEA

This will be adjusted in the revised version.